

Adaptive Initial Blocks for Improving Gradient-Match and Side-Match Vector Quantization of Images

Hsuan T. Chang, Member SPIE, and Yann H. Pan

Photonics and Information Laboratory
Department of Electrical Engineering
National Yunlin University of Science and Technology
Touliu Yunlin, 64045 Taiwan ROC
Email: htchang@pine.yuntech.edu.tw

Abstract

The selection of the initial blocks is one of the important issues in the finite-state vector quantizers (FSVQs) for images. Conventional FSVQs use the blocks located at fixed positions as the initial blocks, which then are coded by the codewords in the super codebook. In this paper, we proposed the *adaptive-initial-block* (AIB) scheme to determine the initial blocks for gradient-match (GM) and side-match (SM) vector quantizers, which are two significant classes of FSVQs. According to the next-state functions used in GMVQs and SMVQs, the blocks with large boundary matching errors in original VQs are selected as the initial blocks. The error propagation effects can be reduced and the coding performance is significantly improved. The simulation results show that the peak signal-to-noise ratios of coded images can be 2 dB higher than that of conventional GMVQs and SMVQs when the state codebook sizes are much smaller than that of the super codebook.

Subject terms: Image coding, adaptive initial blocks, finite-state vector quantization, block boundary, gradient match, side match.

October 29, 2003

1 Introduction

Vector quantization (VQ) is an efficient technique for image compression, especially for the case of very low bit rate coding. It has been dramatically developed since its invention in 1980 for speech coding¹ and in 1984 for image coding.² Recently, the finite-state vector quantizers (FSVQs)³ were proposed to improve the ordinary/memoryless VQ techniques. The block diagram of FSVQs for images is shown in Fig. 1. The main idea is that the previously coded blocks $\{\hat{x}_{i-1}, \hat{x}_{i-2}, \dots, \hat{x}_{i-j}\}$ are buffered and used as the input of the next-state function to determine the corresponding state s_i of the current block. The state s_i points to a state codebook SC_i , which is much smaller than the original super codebook. To encode an input vector x_i , the encoder finds the current state $s_i = f(\hat{x}_{i-1}, \hat{x}_{i-2}, \dots, \hat{x}_{i-j})$ and then searches the state codebook SC_i , not the super codebook, to find the corresponding codeword. The selected codeword may not be equal to the closest codeword that is selected by fully searching the super codebook. Compared with the ordinary VQ schemes, the FSVQs can achieve a higher compression ratio while the image quality is only negligibly degraded.

Two important issues are considered to improve the coding performance of FSVQs: (1) More efficient design for the next-state function. That is, finding the algorithms for constructing better state codebooks. (2) The better selection of the initial blocks. That is, finding the suitable image blocks that can be coded by the use of the super codebook to reduce the coding error. There were several algorithms for designing the next-state function for FSVQs.³⁻⁶ It seems that most of the algorithms are difficult to handle spatial contiguity in images. In attempt to force the encoder to optimize the edge contiguity across block boundaries without doing explicit edge detection, Kim proposed the side match vector quantizers (SMVQs) and overlap match vector quantizers (OMVQs),⁵ which are two classes of FSVQs. Recently, we have also proposed another two classes of FSVQs, named the gradient match vector quantizers (GMVQs) and gradient and overlap match vector quantizers (GOMVQs),⁶ which can outperform the SMVQs and OMVQs, respectively. They can be

drastically improved when they are used together with variable length noiseless coding.^{5,6}

For the issue of the selection of initial blocks, three common schemes shown in Fig. 2 have been proposed. First of all, the image blocks located in the first row and first column (shown in Fig. 2(a)) are selected as the initial blocks. Since the encoding order the image blocks is from top to down and left to right, thus the boundary pixels of the previously encoded blocks in the northern and western sides can contribute the construction of the state codebook for the current block. Then the state codebooks of the remaining blocks are determined by choosing the codewords that result in less boundary matching error between the current block and the western and northern blocks. As shown in Fig. 2(b), an alternative selection of the initial blocks for FSVQs was proposed by Chang and Chen.⁷ In this scheme, the initial blocks are located at the diagonal (45° or 135°) in an image because the diagonal blocks may carry more important information than that shown in Fig. 2(a). The encoding order is not the same as that shown in the previous schemes. Different borders are used for calculating the boundary matching errors of the blocks in the two separate regions apart by the diagonal. For the blocks in the upper-triangle region, the eastern and the southern boundaries with the previously coded blocks are used. On the other hand, for the blocks in the lower-triangle region, the western and the northern boundaries are used. Another arrangement of the initial blocks is shown in Fig. 2(c), in which the initial blocks are selected with a regular interleaving arrangement with, for example, 2 : 1 horizontally and vertically sampling from the image blocks.⁸ Two and more block boundaries can be used in the next state function to improve the coding performance. In this method, however, the use of a large number of initial blocks will greatly increase the bit rate. To reduce the bit rate, some special entropy coding schemes should be employed.

The selection of the initial blocks in the methods shown above is *image-independent*. That is, their positions are fixed and cannot be adopted by the image content. Because the initial blocks are coded with the super codebook, the minimal distortion can be guaranteed.

Since the contents of images may vary a lot, the selection of the initial blocks should be adaptive. On the other hand, the initial blocks are coded by the super codebook rather than the state codebook. They should be selected from the blocks with the least property that used for designing the next-state function. For example, the side match and the gradient match criteria are used in the next-state functions for SMVQs and GMVQs, respectively. Another important concern of FSVQs is the error propagation problem when the coded blocks are much different from the original blocks. The previously coded blocks with large error may result in constructing an inefficient state codebook, which will further degrade the coding performance. Figure 3(a)–(d) shows the original Lena and Peppers images and a given number (for example, 372 is used in our simulation) of the blocks with large mean absolute errors (MAEs) in the image decoded by the conventional GMVQs. The initial blocks are selected as that shown in Fig. 2(a). As shown in Figs. 3(c) and 3(d), many blocks locate at the edges and texture parts in the images. Some error propagation effects appear as the connected groups of blocks. On the other hand, few blocks locate at the first row and column, which obviously is inadequate in selecting the initial blocks. Therefore, it is desired to adaptively select the initial blocks such that the number of the blocks with large MAE errors can be significantly reduced. Based on the reasons shown above, the initial blocks should be determined in an *image-dependent* perspective to improve the coding performance.

In this paper we propose the *adaptive-initial-block* (AIB) scheme, which employs the *boundary gradient match* (BGM) or the *boundary side match* (BSM) criteria to determine the initial blocks for GMVQs and SMVQs. The BGM and BSM methods have been successfully employed in the state codebook design of GMVQs and SMVQs, respectively. The image blocks with large BGM or BSM errors are selected as the initial blocks and then coded by the original VQ scheme. For the right-hand side block of the initial block, the state codebook is constructed by choosing the codewords with the *large* BGM or BSM errors from the super codebook. For the remainder of the blocks, their state codebooks are constructed

by choosing the codewords resulting in the *less* BGM or BSM errors with the neighboring blocks from the super codebook. Since the blocks that result in higher BGM or BSM errors are coded by the use of the super codebook, the minimal coding error can be guaranteed. From the simulation results, the peak signal-to-noise ratios (PSNRs) of the coded images are significantly improved from that in conventional GMVQs and SMVQs under the same bit rates.

2 Adaptive-Initial-Block (AIB) Scheme

The flow charts of the encoder and the decoder in the proposed AIB-based GMVQs and SMVQs are shown in Fig. 4. To determine the adaptive initial blocks, the input image blocks are coded with full search VQ in advance. Then the BGM or BSM criteria are applied to all dequantized blocks. The adaptive initial blocks are composed of two parts: (1) The fixed part – the diagonal blocks of the image; (2) The image-dependent part – a given number of the blocks whose BGM or BSM errors are larger than other image blocks. The reason we choose the diagonal blocks is to guarantee that at least two previously coded blocks can be used for measuring the BGM or BSM errors to construct the state codebook for the current block. Since the initial blocks are separated by the diagonal blocks and their positions are image dependent, different conditions will be considered while constructing the state codebook. (It will be described in Subsection 2.3.) Their positions in the image and their indices in the super codebook are recorded. Since the initial blocks may arbitrary distribute in the image, their eastern blocks are then coded. Finally, the residual blocks are coded with the state codebooks constructed by the conventional ways in GMVQs and SMVQs. In the decoder, a symmetric architecture is employed for reconstructing all the blocks by the use of the received positions of the initial blocks and the indices. The detailed procedures of the proposed AIB-based GMVQs and SMVQs are described by the following subsections.

2.1 BGM and BSM Criteria

To determine the initial blocks, first of all the image is coded by the use of the ordinary full-search VQ technique. Next, the BGM or BSM error between two adjacent blocks is calculated. The error calculation for the vertical or the horizontal boundary can be accepted. The labeled area in Fig. 5 corresponds to the pixels that are used to determine the BGM and BSM errors in the vertical boundary of two blocks \mathbf{x} and \mathbf{l} . Suppose that all image blocks are of size m by n . The BGM and BSM errors of two neighboring blocks \mathbf{x} and \mathbf{l} along the vertical boundary are defined by⁶

$$E_{\text{gm}} = \sum_{i=1}^m (|l_{i,n-1} - 2l_{i,n} + x_{i,1}| + |l_{i,n} - 2x_{i,1} + x_{i,2}|)^2, \quad (1)$$

and

$$E_{\text{sm}} = \sum_{i=1}^m (x_{i,1} - l_{i,n})^2, \quad (2)$$

respectively. Here $x_{i,j}$ and $l_{i,j}$ denote the $(i, j)^{\text{th}}$ pixel in the blocks \mathbf{x} and \mathbf{l} , respectively. A threshold value E_{th} can be set to choose the blocks resulting in large boundary matching errors. Instead, a given number (for example, the number 500 is used in our computer experiment) of blocks resulting in larger errors than others can be defined. If the BGM or BSM error of two adjacent blocks is larger than the threshold value E_{th} , the block at the left-hand side is selected as the initial block. Then these initial blocks are coded with the super codebook. In fact, this has been done in the full-search VQ. In addition to the indices of the initial blocks, their positions should also be recorded and transmitted to the decoder. For the block at the right-hand side, the state codebook is constructed by choosing the boundary matching errors that are larger than the threshold value.

2.2 Coding of Initial Blocks Position

Since the initial blocks are adaptively selected, the positions of the initial blocks should be recorded and transmitted to the decoder. The positions of the initial blocks are recoded by the use of the run-length coding technique.⁹ Note that the blocks located at the diagonal of

the image are fixed for all images. Therefore, it is not necessary to record the positions of the diagonal blocks unless that the initial blocks are located at the diagonal. The map of the initial blocks is of size 128 by 128 when the image is of size 512 by 512 and the blocks are of size 4 by 4. For the blocks belonging to the initial blocks, they are denoted by the bit ‘1.’ On the other hand, the residual blocks are denoted by the bit ‘0’ in the map. To reduce this overhead for denoting the positions of the initial blocks, the bit map is further encoded by the run length coding. The bit rate can be significantly reduced after the entropy coding because the given number of the initial blocks are usually small, that is, most of the bits in the map are ‘0’s.

2.3 State Codebook Design of Residual Blocks

Excluding the initial blocks, the residual blocks in the image are divided into two types:

- (1) The eastern neighboring blocks of the initial blocks;
- (2) The blocks that are not directly neighboring to any initial block at the eastern side.

The design methods of the state codebooks for these two types of blocks are different. For the blocks in type (1), the vertical boundary matching errors between the initial blocks and the codewords in the super codebook are measured at first. If we have determined a given number of the initial blocks in advance, the minimum matching error E_{\min} can be obtained and is used as the threshold value E_{th} for determining the number of the codewords in the corresponding state codebook. The state codebooks are constructed by at least choosing the N' codewords whose matching errors are larger than the error E_{\min} . To construct an efficient state codebook, we can take more codewords from the super codebook such that the number of the codewords to be the powers of two. That is, the number of the codewords in the state codebook should be $2^{\lceil \log_2 N' + 1 \rceil}$.

For the blocks that do not connect to the initial blocks in the eastern side, the state codebooks are constructed by choosing the N codewords with smaller matching errors than others from the super codebook. Here the number N is a pre-defined number of the code-

words in the state codebook. Note that the determination of the BGM and BSM errors should depend on the connecting side of two neighboring blocks. That is, both the vertical and horizontal directions are possible. On the other hand, the state codebook is constructed using the BGM or BSM errors from at least two sides. To guarantee this condition, the initial blocks should include the diagonal blocks. In addition to two sides, three and four sides are also possibly used to determine the BGM and BSM errors in constructing the corresponding state codebooks. Basically, better quality can be expected if more sides are used here.

Figure 6 shows the examples of different conditions for the current block. The blocks are classified as two parts by using the diagonal blocks. The black blocks denote the initial blocks with large BGM or BSM errors, while the gray blocks denote the diagonal ones. Both types of blocks may overlap. Consider the two classes of the blocks: the blocks R_1 – R_8 shown in Fig. 6(a) located at the lower-right part of the image and the blocks L_1 – L_8 shown in Fig. 6(b) located at the upper-left part of the image. As shown in Figs. 6(a) and 6(b), the state codebooks of the blocks $\{R_1, R_9\}$ and $\{L_1, L_8\}$ are designed based on the methods used in conventional GMVQs or SMVQs. For the blocks $\{R_2, R_4, R_7\}$ and $\{L_2, L_4, L_5\}$, which are directly located at the eastern side of a initial block, their state codebooks are constructed by selecting the codewords whose BGM or BSM errors are greater than the threshold value E_{\min} . For the blocks $\{R_3, R_5\}$ and $\{L_3, L_6\}$, more than two previously coded blocks can contribute to the construction of the state codebooks.

After the state codebook has been constructed, each block in both types is encoded by the index by the use of the nearest neighboring search method. Their indices are recorded and then transmitted to the decoder. In decoder, the initial blocks will be decoded at first and then the residual blocks are decoded with the corresponding state codebooks that are constructed from the similar procedures in the encoder.

2.4 Variable Length Noiseless Coding

Entropy coding¹⁰ has been extensively studied to reduce the average number of symbols sent while suffering no loss of fidelity. Given a class of sources such as an image, the channel symbols assume a certain probability distribution. Because of the high correlation in images and the ordering in each state codebook by the matching error, we can guess that the channel symbol distribution assumes a monotonically decreasing trend. When codebooks are fixed, the decreasing trend varies from image to image according to the spatial correlation of images. According to this monotonically decreasing trend, Kim proposed a noiseless code⁵ which is basically the Huffman code designed for the stair case approximation to fast decaying distributions. Based on the noiseless code he proposed, both the SMVQs and GMVQs have shown a great reduction in bit rate.^{5,6} In order to compare with the conventional SMVQs with GMVQs on bit rate reduction, we also apply the variable length noiseless coding technique on the proposed AIB-based GMVQs and SMVQs techniques.

3 Experimental Results

In computer simulation, the block size is 4 by 4 and four images: Peppers, Lady, Building, and F-16 (with size 512×512 and 8-bit grayscale resolution) shown in Figs. 3(b) and 7(a)–(c) are used as the training images for VQ. The super codebooks of various sizes are generated by applying the LBG algorithm.¹ The coding performance of the proposed scheme is compared with those of the ordinary VQ, the SMVQs, and the GMVQs. Because the peak value of the grayscale levels in an image is 255, the PSNR of a decoded image is defined as

$$\text{PSNR} = 10 \log_{10} \frac{512^2 \cdot 255^2}{\sum_{i=1}^{512} \sum_{j=1}^{512} [f(i, j) - f'(i, j)]^2} \text{ dB}, \quad (3)$$

where $f(i, j)$ and $f'(i, j)$ denote the $(i, j)^{\text{th}}$ pixel value in the original and decoded images, respectively. Note that the bit rate is expressed by bits per pixel (bpp).

To calculate the bit rate of the coded image, four different parts are considered.

(1). The number of bits I_{map} for the map denoting the positions of the initial blocks.

(2). The number of bits I_{ini} for the indices of the initial blocks. That is, $I_{\text{ini}} = N_{\text{ini}} \cdot \log_2 N_s$, where N_s denotes the number of codewords in the super codebook.

(3). The number of bits I_{nei} for the indices of the neighboring blocks of the initial blocks with large BGM or BSM errors. That is, $I_{\text{nei}} = \lfloor \log_2 N' + 1 \rfloor$.

(4). The number of bits I_{res} for the indices of the residual blocks.

Therefore the final bit rate can be calculated as

$$I = \frac{I_{\text{map}} + I_{\text{ini}} + I_{\text{nei}} + I_{\text{res}}}{512^2} \text{ bpp.} \quad (4)$$

Note that the bits required to denote threshold value E_{min} is not considered here since it only increases negligible bit rate.

In determining the initial blocks of the four test images, the given number of the initial blocks is 500 (including the 128 diagonal blocks). The determined initial blocks for two test images (Lena and Peppers) with the BGM criterion are shown in Fig. 8(a) and 8(b). (Similar results is obtained for BSM criterion.) Obviously, the distributions of the initial blocks (excluding to the diagonal part) for different images are image dependent and quite similar to that shown in Fig. 2. The initial blocks with large boundary matching errors are coded with the super codebook and thus their distortions can be reduced.

During our computer experiments, the super codebooks are of sizes 256, 512, 1024, and 2048. On the other hand, the state codebooks are of sizes 16, 32, 64, 128, and 256. Figure 9(a) and 9(b) shows the rate-PSNR comparisons of the two images among the ordinary VQ, GMVQs, and the AIB-based GMVQs. Here ‘GMVQ(1)’ and ‘GMVQ(2)’ denote the GMVQs with the fixed initial blocks located in the diagonal (Fig. 2(b)) only and the first row and first column (Fig. 2(a)), respectively. Similar results for the rate-PSNR comparisons of the four images can be obtained among the ordinary VQ, SMVQs, and the AIB-based SMVQs. Therefore, the performance of the proposed scheme significantly improves the PSNR performance of conventional VQs, GMVQs, and SMVQs, especially in the cases that the state codebook sizes are much smaller than that of the super codebook. The PSNR is even higher

than 1 dB for the test images when the state codebook size is 16. In addition to the Lena and Peppers images, we also test the proposed method for other two images, Building and F-16, shown in Fig. 7(b) and 7(c). According to the simulation results, higher coding gains are obtained for the Lena, Peppers, and F-16 images, which are less complicated than the Building image. Therefore, it is expected that the proposed method is more worthwhile for the less complicated images.

We next investigate the probability distributions of the channel symbols for different quantizers. Consider the Lena image that is not within the training images. The bit rate reduction has been proved when applying the variable length noiseless coding on SMVQs and GMVQs.⁶ If the probability distributions are more concentrated in the first index, then more bit rate reduction could be possible. Tables 1 and 2 show the probabilities of the channel symbol (index) is ‘1’ for the proposed AIB-based GMVQs and SMVQs, respectively. The super codebooks are of sizes from 256 to 2048 and the state codebooks are of sizes from 16 to 256. As shown in both tables, the probabilities under different super codebook sizes for the AIB-based GMVQs and SMVQs are very similar. The probabilities (0.39 and 0.38) in the proposed AIB scheme are higher than that (0.34 and 0.32) shown in Ref. [6] when the super codebook size is 256 and the state codebook size is 64. Therefore, further bit rate reduction can be achieved when the entropy coding is used in the proposed AIB-based GMVQs and SMVQs.

Here we make comparisons between (1) the AIB-based GMVQs and the conventional GMVQs, (2) the AIB-based SMVQs and the conventional SMVQs. Figure 10(a) and 10(b) shows the performance comparison between the AIB-based GMVQs (dot lines) and the conventional GMVQs (dash lines). Both results with the variable length noiseless coding technique are also shown. The curve pair represents the coding results with and without using the variable length noiseless coding technique. Here the bit reductions in GMVQs and SMVQs are quite similar and very significant. With the variable length noiseless code

technique, the AIB-based GMVQs and SMVQs still outperform the conventional GMVQs and SMVQs. The PSNR values in the proposed AIB-based GMVQs and SMVQs can be 2 dB better than that in conventional GMVQs and SMVQs when the same bit rate in the case that the state codebook is of size 16. Figure 11 shows the decoded Lena images from the proposed AIB-based and conventional GMVQs under this case. The proposed AIB scheme greatly enhances the image quality, especially for the high contrast (eyes and hat edges) and the high frequency (hair and texture) contents.

In Section 1, we determine the 372 blocks with large MAE errors in conventional GMVQs and SMVQs. Here the 372th MAE value of each image is used as the threshold value for examining the image decoded by the proposed AIB-based GMVQs and SMVQs. Table 3 summarizes the numbers of the blocks with MAE values larger than that of 372th coded block in conventional GMVQs and SMVQs. Obviously the numbers of blocks are greatly reduced and thus the PSNR of the decoded image is improved, which is consistent with our experimental results.

We have shown that the proposed AIB-based GMVQs and SMVQs can outperform conventional GMVQs and SMVQs in the image coding framework, respectively. However, the disadvantages in the proposed AIB-based GMVQs and SMVQs are the additional computation required for determining the initial blocks and the complicated next-state functions for different types of blocks described in Section 2.3. The increased complexity for choosing the initial blocks is basically the required computation in the original VQ scheme. Only the encoder suffers this additional computation, which is proportional to the size of super codebook. Since the algorithm of original VQ scheme is very straightforward, the extra coding time is negligible. On the other hand, the state codebooks can be off-line designed once the super codebook has been generated and before the encoding/decoding stage. The payment is the increased memory size for storing the next-state functions. That is, the next-state functions can be realized by table lookup to speed up the process. For the most of the prac-

tical applications, the most significant concern for image compression is the decoding speed. Although the encoding of the proposed method requires more computation, the decoding speed is comparable to that of the conventional GMVQs and SMVQs.

There should be other methods for choosing initial blocks. The proposed AIB scheme may not be optimal for all FSVQs. However, we can guarantee that the initial blocks determined by the GM and SM criteria are optimal for GMVQs and SMVQs, respectively. On the other hand, we don't think that some twisting in Eqs. 1 or 2 can significantly improve the results further.

4 Conclusion

In this paper, the AIB scheme based on the BGM and BSM criteria is proposed to adaptively determine the initial blocks for conventional GMVQs and SMVQs. The error propagation effects are reduced because the determined initial blocks basically locate at the positions of the blocks with large coding error in conventional GMVQs and SMVQs. The state codebooks of the residual blocks are constructed based on the adaptively selected initial blocks. Computer experiments show that the rate-PSNR performances of conventional GMVQs and SMVQs for images are significantly improved, especially for the cases of the small state codebooks. Moreover, the bit rate is further reduced when the entropy coding scheme such as the variable length noiseless coding is applied on the channel symbols. In addition to FSVQs, the potential applications of the proposed AIB scheme could be the algorithms that require the selection of the initial conditions, such as the codebook training in VQ techniques and optimization problems in engineering, etc.

Acknowledgment

This research was partially supported by the National Science Council, Taiwan, under contracts NSC 90-2213-E-224-029 and NSC 92-2213-E-224-047.

References

- [1] Y. Linde, A. Buzo, and R. Gray, “An algorithm for vector quantization design,” *IEEE Trans. On Communications*, **28**(1), 84–95 (1980)
- [2] R. M. Gray, “Vector quantization,” *IEEE ASSP Mag.*, 4–29 (1984)
- [3] A. Gersho and R. M. Gray, *Vector Quantization and Signal Compression*. Boston, MA: Kluwer (1992)
- [4] N. Nasrabadi and S. Rizvi, “Next-state functions for finite-state vector quantization,” *IEEE Trans. On Image Processing*, **4**(12), 1592–1601 (1995)
- [5] T. Kim, “Side match and overlap match vector quantization for images,” *IEEE Trans. On Image Processing*, **1**(2), 170–185 (1992)
- [6] Hsuan T. Chang, “Gradient match vector quantizers for images,” *Optical Engineering*, **39**(8), 2046–2057 (2000)
- [7] T.-S. Chen and C.-C. Chang , “A new image coding algorithm using variable-rate side-match finite-state vector quantization,” *IEEE Transactions on Image Processing*, **6**(8), 1185–1187 (1997)
- [8] H.-C. Wei, P.-C. Tsai, and J.-S. Wang, “Three-sided side match finite-state vector quantization,” *IEEE Trans. on Circuits and Systems for Video Technology*, **10**(1), 51–58 (2000)
- [9] R.C. Gonzalez, *Digital Image Processing*, Chapter 6, 354–355, Addison Wesley (1993)
- [10] N.S. Jayant and P. Noll, *Digital Coding of Waveforms - Principles and applications to speech and video*, Prentice Hall International Inc. (1984)

Table 1: The probabilities for the channel symbol (codeword index) ‘1’ in the proposed AIB-based GMVQs with different sizes of the super codebook.

Super codebook size	State codebook size				
	16	32	64	128	256
256	0.388	0.389	0.390	0.390	0.390
512	0.252	0.249	0.250	0.251	0.251
1024	0.190	0.185	0.184	0.184	0.185
2048	0.136	0.122	0.124	0.125	0.125

Table 2: The probabilities for the channel symbol (codeword index) ‘1’ in the proposed AIB-based SMVQs with different sizes of the super codebook.

Super codebook size	State codebook size				
	16	32	64	128	256
256	0.381	0.380	0.381	0.381	0.381
512	0.266	0.262	0.263	0.264	0.264
1024	0.210	0.204	0.203	0.202	0.203
2048	0.141	0.132	0.131	0.129	0.130

Table 3: The numbers of the blocks with MAE values larger than that of 372th coded block in conventional GMVQs and SMVQs, in which the sizes of the super codebook and the state codebook size are 256 and 16, respectively.

Image	Lena	Peppers	Lady	F-16	Building
AIB-based GMVQs	180	209	260	165	231
	↓ 52%	↓ 44%	↓ 30%	↓ 56%	↓ 38%
AIB-based SMVQs	144	190	217	159	177
	↓ 61%	↓ 49%	↓ 42%	↓ 57%	↓ 52%

Figure Captions:

Figure 1: The block diagram of the encoder and decoder in FSVQs.

Figure 2: Three different methods for selecting the fixed initial blocks in conventional FSVQs.

Figure 3: The original (a) Lena and (b) Peppers images and their corresponding 372 coded blocks with large MAE distortion in conventional GMVQs, which are shown in (c) and (d), respectively.

Figure 4: The flow charts of the proposed AIB-based GMVQs and SMVQs: (a) encoder; (b) decoder.

Figure 5: The pixels that are used to determine the BGM and BSM errors at the block boundary. (In this case, $m = 4$ and $n = 4$.)

Figure 6: The possible conditions for the currently coded blocks in the proposed method: (a) lower right part; (b) upper left part.

Figure 7: Three training images: (a) Lady, (b) Building, and (c) F-16.

Figure 8: The 500 initial blocks determined by the BGM criterion for (a) Lena and (b)Peppers images.

Figure 9: Comparison of the rate-PSNR results for original VQs, conventional GMVQs(1) and GMVQs(2), and the proposed AIB-based GMVQs.

Figure 10: Comparison of the entropy coding results for the proposed AIB-based GMVQs and SMVQs and the conventional GMVQs and SMVQs. The super codebook is of size 1024.

Figure 11: Decoded Lena images of the proposed AIB-based GMVQs and the conventional GMVQs: (a) 29.38 dB, 0.251 bpp; (b) 26.80 dB, 0.241 bpp. The super codebook and the state codebook are of sizes 1024 and 16, respectively.

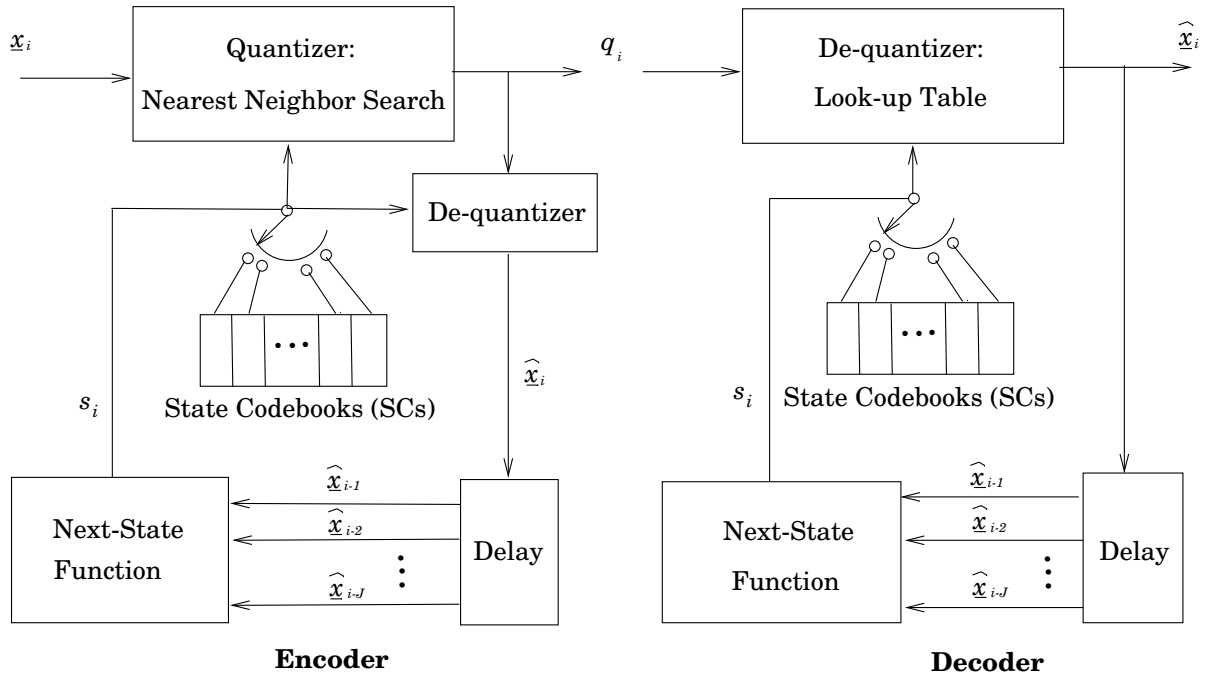


Figure 1: The block diagram of the encoder and decoder in FSVQs.

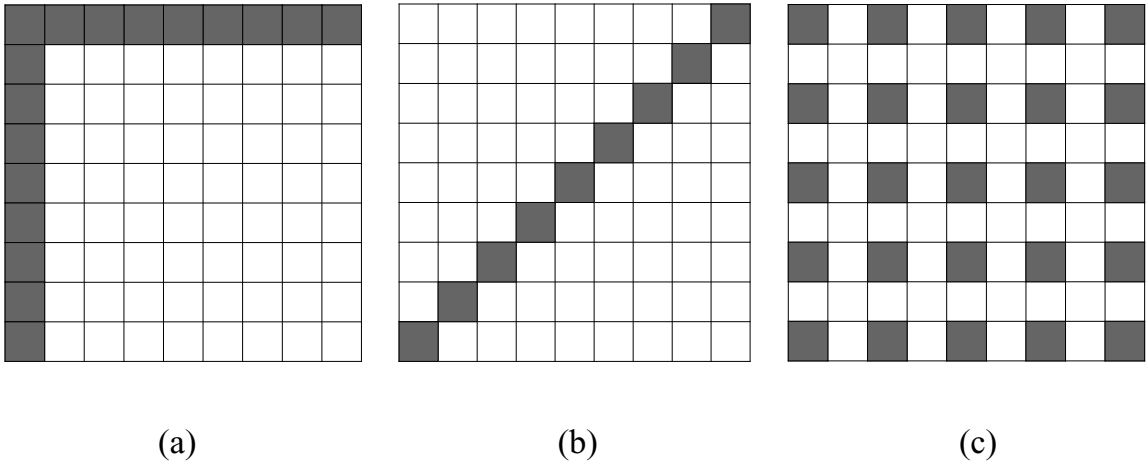


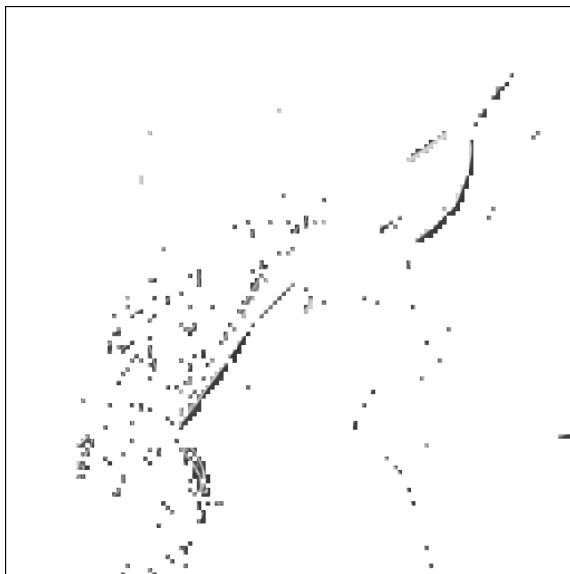
Figure 2: Three different methods for selecting the fixed initial blocks in conventional FSVQs.



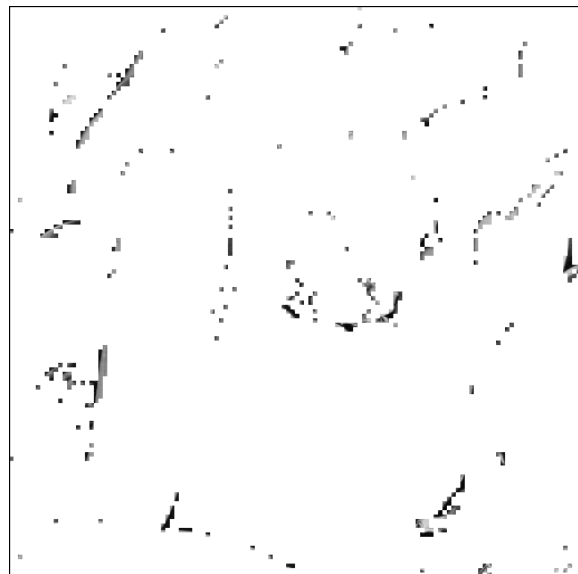
(a)



(b)



(c)



(d)

Figure 3: The original (a) Lena and (b) Peppers images and their corresponding 372 coded blocks with large MAE distortion in conventional GMVQs, which are shown in (c) and (d), respectively.

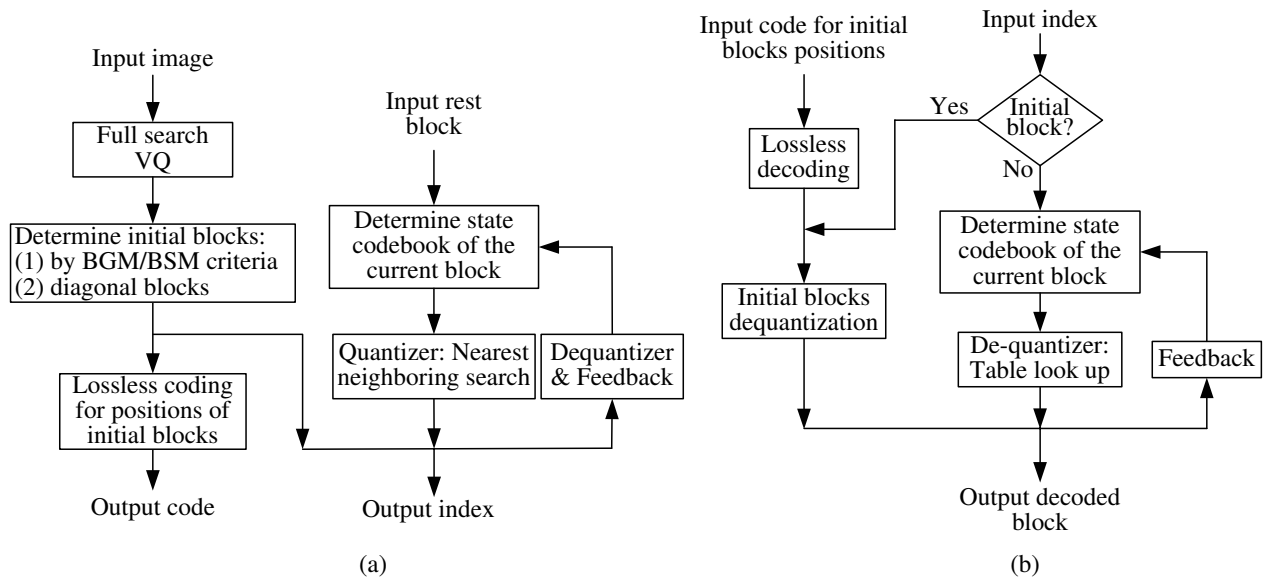


Figure 4: The flow charts of the proposed AIB-based GMVQs and SMVQs: (a) encoder; (b) decoder.

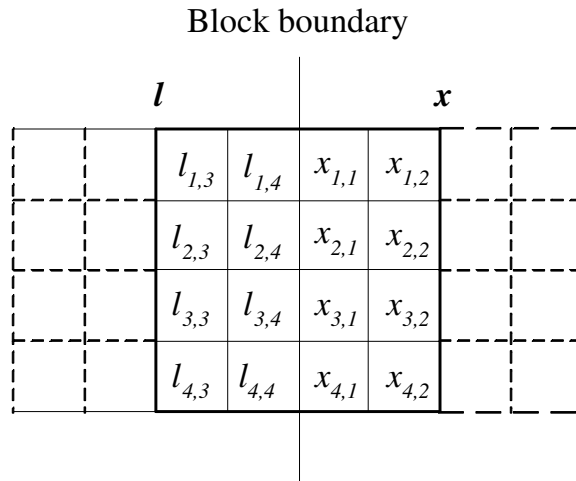


Figure 5: The pixels that are used to determine the BGM and BSM errors at the block boundary. (In this case, $m = 4$ and $n = 4$.)

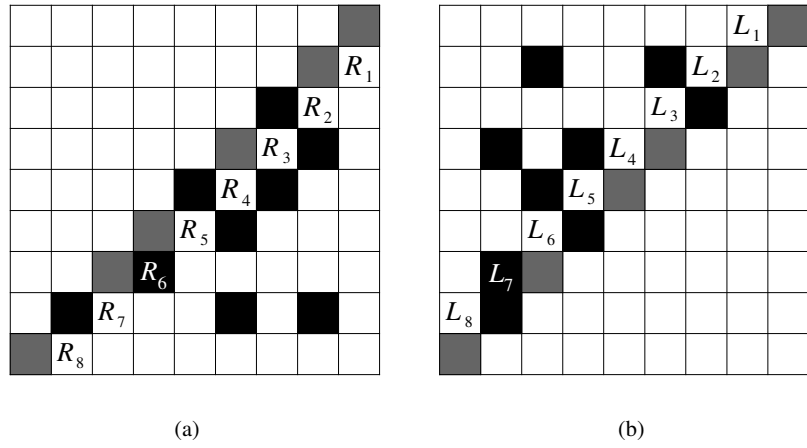


Figure 6: The possible conditions for the currently coded blocks in the proposed method: (a) lower right part; (b) upper left part.



(a)

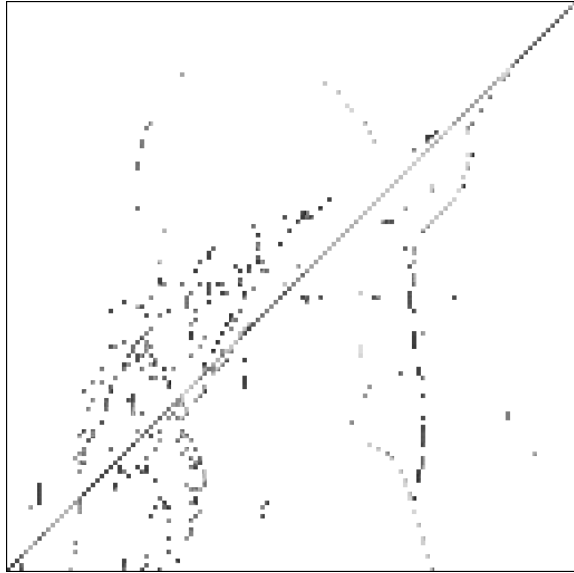


(b)

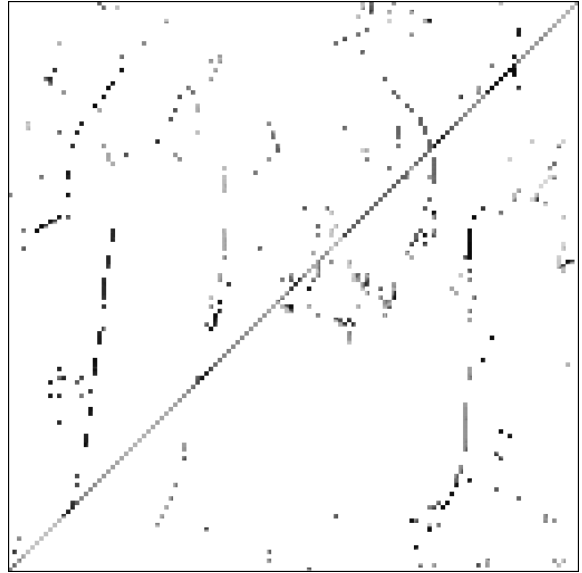


(c)

Figure 7: Three training images: (a) Lady, (b) Building, and (c) F-16.



(a)



(b)

Figure 8: The 500 initial blocks determined by the BGM criterion for (a) Lena and (b)Peppers images.

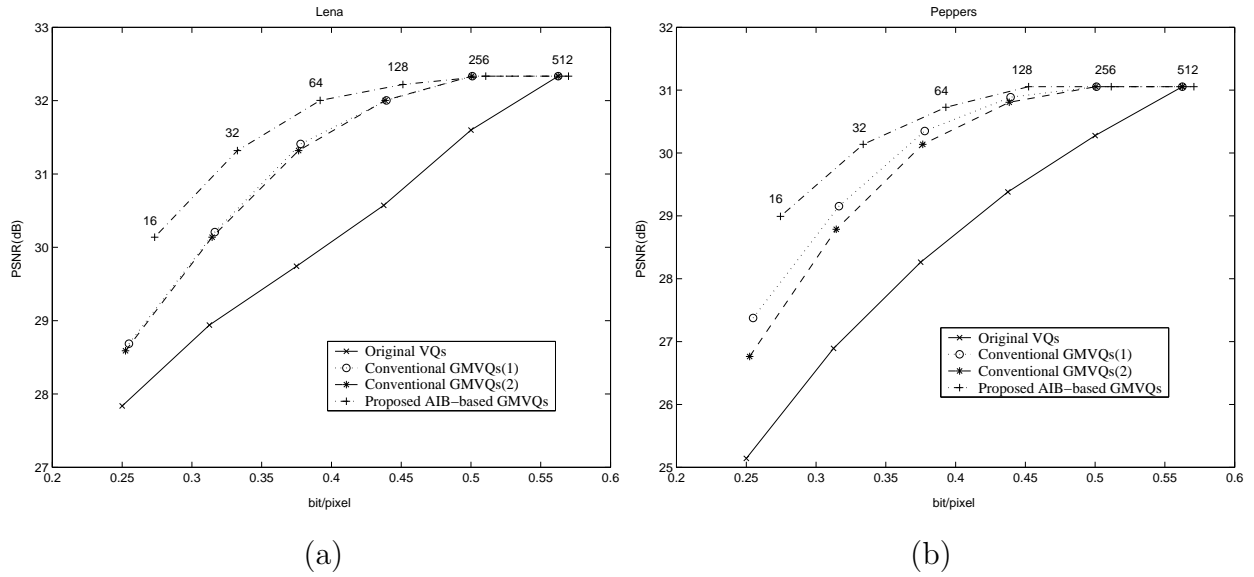
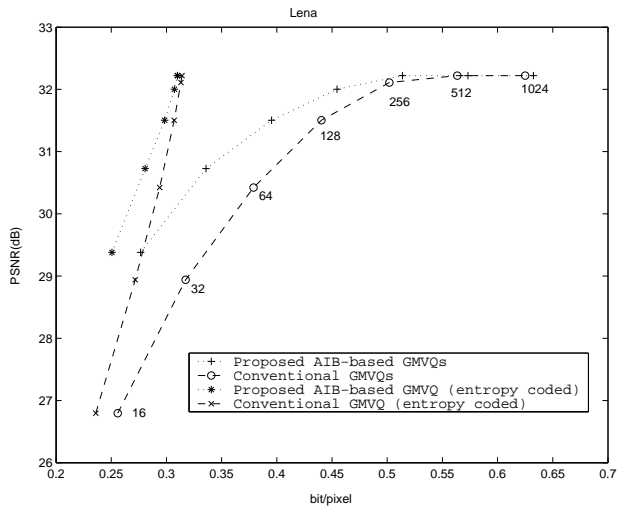
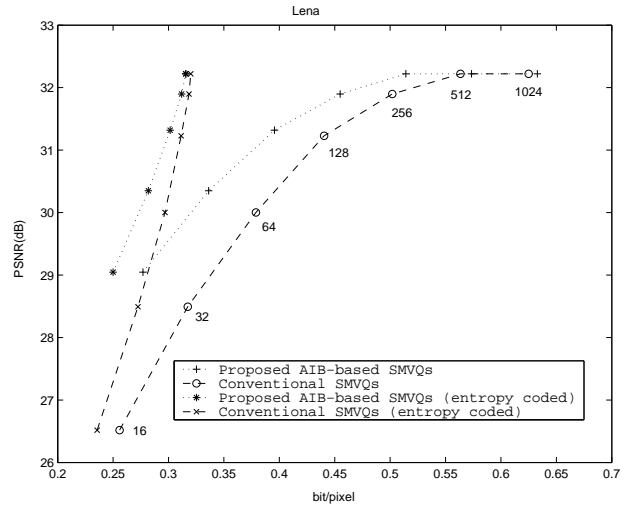


Figure 9: Comparison of the rate-PSNR results for original VQs, conventional GMVQs(1) and GMVQs(2), and the proposed AIB-based GMVQs.



(a)



(b)

Figure 10: Comparison of the entropy coding results for the proposed AIB-based GMVQs and SMVQs and the conventional GMVQs and SMVQs. The super codebook is of size 1024.



(a)

(b)

Figure 11: Decoded Lena images of the proposed AIB-based GMVQs and the conventional GMVQs: (a) 29.38 dB, 0.251 bpp; (b) 26.80 dB, 0.241 bpp. The super codebook and the state codebook are of sizes 1024 and 16, respectively.